ChemComm

Continuum of Covalent to Intermolecular Bonding in the Halogen-Bonded Complexes of 1,4-Diazabicyclo[2.2.2]octane with Bromine-Containing Electrophiles

Journal:	*ChemComm*
Manuscript ID	CC-COM-06-2018-004629.R1
Article Type:	Communication

Journal Name

COMMUNICATION

Continuum of Covalent to Intermolecular Bonding in the Halogen-Bonded Complexes of 1,4-Diazabicyclo[2.2.2]octane with Bromine-Containing Electrophiles

Received 00th January 20xx,
Accepted 00th January 20xx

DOI: 10.1039/x0xx00000x

www.rsc.org/

Craig Weinberger,[a] Rachel Hines,[a] Matthias Zeller[b] and Sergiy V. Rosokha*[a]

A gradual change of Br···N bond lengths and strengths from the values typical for intermolecular associates to that characteristic of a covalent bond was observed in the series of the halogen-bonded complexes. This continuum reveals fundamental relationship between the limiting types of bonding and implies the onset of covalency in the intermolecular interactions.

The recent development of supramolecular chemistry brought about new aspects to the discussion of the nature and limits of the chemical bond.[1] While supramolecular interactions are commonly referred to as non-covalent bonding, many works suggest that some of them comprise substantial covalent components.[2-4] Also, the preparation of supramolecular complexes with short interatomic distances[5] and the expansion of the limits of the covalent bond length,[6] diminished the separation between inter- and intramolecular bonding. However, there is still a significant gap between the typical covalent bond lengths and intermolecular distances.

To test the feasibility of a gradual transition between covalent and intermolecular bonding, we studied halogen-bonded (XB) complexes of bromo-substituted R-B electrophiles (Scheme 1) with 1,4-diazabicyclo[2.2.2]octane (DABCO). The interest in halogen bonding has grown considerably during the last two decades and a large number of associates with XB lengths much shorter than the van der Waals separations were prepared.[7,8] In particular, very strong and relatively weak complexes of DABCO with bromo-substituted molecules showing Br···N separations of ~2.3 Å and ~2.9 Å, respectively, were reported.[9-11] Yet, there is a more than 0.4 Å break between the Br···N distances in the strongly interacting complexes and the covalent N–Br bond length (~1.85 Å[12]), as well as the interatomic distances in the weak associates. To establish a continuum of bond lengths, as well as thermodynamic and spectral features of the XB associates, we characterized complexes between DABCO and an extended series of the R–Br electrophiles, as follows.

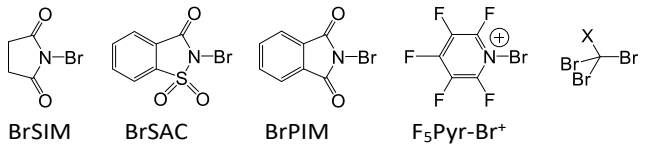

Scheme 1. Structures and abbreviations of some of the R–Br electrophiles (X = H, F, Br, CN, NO_2, $CONH_2$, $COCBr_3$, etc.).

As illustrated in Fig.1, addition of DABCO to the solutions of R-Br electrophiles in acetonitrile resulted in the appearance of absorption bands in the 200 - 400 nm range. Concentration and temperature dependence of intensities of these bands measured with various R–Br molecules (Figures S1 – S7 in the ESI) confirmed that their appearance is related to the formation of 1:1 complexes (eq 1):§

R-Br + DABCO ⇌ [R-Br, DABCO] (1)

Treatments of the UV-Vis data (see the ESI for details) afforded formation constants and spectral characteristics of the [R-Br, DABCO] complexes (Table 1).

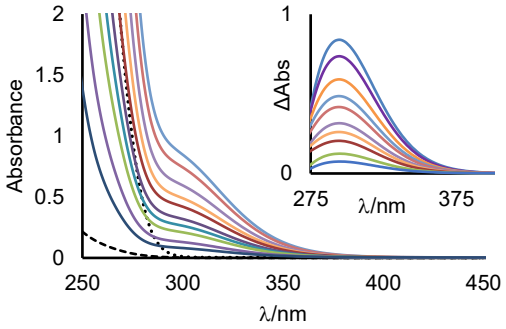

Figure 1. Spectral changes occurring upon addition of DABCO to the solution of R-Br (R-Br = CBr_3F). Dot and dashed lines show spectra of the individual DABCO and R-Br solutions, respectively. Insert: spectra of the complex obtained by the subtraction of the absorption of components from the spectra of their mixtures.

[a] Department of Chemistry
Ball State University
Muncie, Indiana 47306 USA
E-mail: svrosokha@bsu.edu
[b] Department of Chemistry
Purdue University
West Lafayette, Indiana 47907, USA.

Electronic Supplementary Information (ESI) available: [details of any supplementary information available should be included here]. See DOI: 10.1039/x0xx00000x

Table 1. Experimental characteristics of the [R-Br, DABCO] complexes.[a]

R-Br	λ, nm	ε, 10^3 $M^{-1}cm^{-1}$	K, M^{-1}
CBr_3H	288	2.8	0.2
CCl_3Br	290	5.0	0.9
CBr_3CONH_2	295	1.7	1.0
CBr_3F	300	4.8	1.1
CBr_3COCBr_3	320	3.0	1.9
CBr_4[b]	313	2.5	3.7
CBr_3NO_2	290	6.0	7.5
CBr_3CN	292	7.2	7.8
BrSIM[b]	253	16.4	424
BrSAC[b]	224	c	c
Br_2	295	c	c

[a] In CH_3CN, 22°C. [b] Ref. [9]. [c] Quantitative measurements of complex formation were hindered by side reactions.

Slow evaporation or cooling of the solutions containing R–Br electrophiles and DABCO resulted in formation of co-crystals suitable for single-crystal X-ray structural measurements.‡ For example, when a solution of DABCO and CBr_3NO_2 in chloroform was cooled from room temperature to 0° C, yellow crystals developed. X-ray structural analysis revealed that the DABCO and CBr_3NO_2 moieties form zigzag chains (Figure 2).

Co-crystallization of DABCO with $CHBr_3$, CBr_3CONH_2 or $CBrCl_3$ molecules resulted in the formation of similar chains (Figures S8 in the ESI). In the crystals with tribromoacetamide or bromoform, however, each DABCO molecule forms a halogen bond with one of its neighbors and a hydrogen bond with another electrophile. In the co-crystals of DABCO with $CBrCl_3$, the molecules of the electrophile are partially disordered, so the bromine substituent shares the positions that are halogen-bonded to the nucleophiles with one of the chlorine atoms. The Br···N separations in these chains are listed in Table 2.

In the co-crystals with CBr_3F, each DABCO molecule is bonded to two electrophiles. In turn, the CBr_3F molecules are bonded either to one, two or three DABCO molecules (Figure S8 in the ESI). The increase of the number of nucleophiles bonded to the CBr_3F electrophile is accompanied by an increase of the XB length from 2.654 Å to 2.764 Å (Table 2).

Pale-yellow co-crystals of dibromine and DABCO comprised both components in a 2:1 molar ratio, as well as CH_2Cl_2 solvate molecules. Each DABCO molecule is bonded to two Br_2 electrophiles (Fig. 3A) and the two short Br···N distances of ~2.16 Å within these complexes are almost equivalent (Table 2).

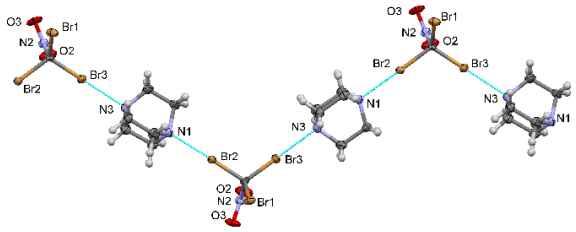

Figure 2. XB chains in the CBr_3NO_2·DABCO co-crystals.

Table 2. The N···Br distances in the R-Br·DABCO co-crystals.[a]

R-Br	$d_{Br\cdots N}$, Å	R_{vdW} (R_{cov}) [a]	Refr
$C_6Br_2F_4$[b]	2.910, 2.894	0.85 (1.57)	[11a]
$CHBr_3$	2.877	0.85 (1.56)	This work
$C_2Br_2F_4$	2.829	0.83 (1.53)	[11b]
CBr_3CONH_2	2.772	0.82 (1.50)	This work
Br-C≡C-CPh_3	2.771 2.833	0.82 (1.50)	[11c]
CCl_3Br	2.714, 2.732	0.80 (1.47)	This work
CBr_4	2.726, 2.735	0.80 (1.47)	[9]
$CFBr_3$	2.654, 2.687, 2.735, 2.741, 2.758, 2.764,	0.80 (1.47)	This work
CBr_3NO_2	2.543, 2.605	0.76 (1.39)	This work
BrSIM	2.332, 2.364, 2.347	0.69 (1.27)	[10a,b]
BrPIM	2.257, 2.322, 2.348	0.68 (1.25)	[10c]
Br_2	2.165, 2.166	0.64 (1.17)	This work
DABCO-Br^{+c}	2.130	0.63 (1.15)	This work

[a] $R_{vdW} = d_{Br\cdots N}/(R_{Br}+R_N)$ and $R_{cov} = d_{Br\cdots N}/R_{NBr}$, where $d_{Br\cdots N}$ is an average Br···N distance in the complex, R_{NBr} = 1.85 Å[12] is N–Br covalent bond length, R_{Br} = 1.85 Å and R_N = 1.55 Å are van der Waals radii of Br and N atoms.[13] [b] 1,4-dibromotetrafluoro-benzene. [c] Fragment of the $[DABCO–Br–DABCO]^+$ analoguous to the R-Br electrophile in the neutral complexes.

Evaporation of a solution containing a mixture of DABCO and N-bromosaccharin resulted in the formation of colorless crystals which comprised $[DABCO–Br–DABCO]^+$ triads (Fig. 3B) and saccharate counter-ions. The triads (which were apparently a product of bromonium transfer) are characterized by two N···Br bond lengths of 2.130 Å. Notably, the Br···N distances in the [Br_2-DABCO–Br_2] and $[DABCO–Br–DABCO]^+$ complexes are much closer to the N–Br covalent bond length of ~ 1.85 Å than to the van der Waals separation of these atoms of 3.40 Å.

The Br···N distances in the XB complexes (Table 2) vary drastically, ranging from 2.13 Å (which is just ~15 % longer than the N–Br covalent bond) to 2.91 Å (which is ~15 % shorter than the van der Waals separation of the bromine and nitrogen atoms). Their formation constants change by over three orders of magnitude (Table 1). To better understand the properties of these complexes, we performed computations on a series of R-Br·DABCO adducts. In addition to the above mentioned complexes, this series included asociates of DABCO with diverse

A

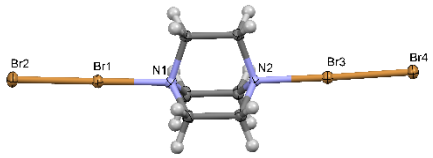

B

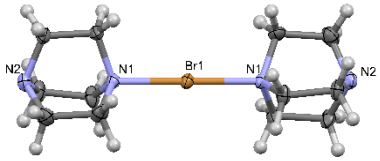

Figure 3. X-ray structures of the [Br_2-DABCO-Br_2] (A) and $[DABCO-Br-DABCO]^+$ (B) complexes.

electrophiles (e.g. CH_3Br, BrF) as well as some cationic analogues of [DABCO-Br-DABCO]$^+$, i.e. [F_5pyr-Br-DABCO]$^+$ and [pyrazine-Br-DABCO]$^+$. All complexes were optimized via DFT (M06-2X/6-311+G(d,p)) calculations (see the ESI). The interatomic Br···N distances, $d_{Br\cdots N}$, and the interaction energies, ΔE, in the optimized complexes are listed in Table 3.

The calculated Br···N distances show a good correlation with the experimental values (R^2 = 0.94, see Figure S10 in the ESI). The values of ΔE show a similar correlation with the free energies of the complex formation measured in acetonitrile (Figure S10 in the ESI). Finally, TD DFT computations of the optimized complexes produced strong absorption bands in the UV-Vis spectra. The wavelengths and intensities of the absorption bands' maxima were reasonably close to the experimental values. All these data confirmed the reliability of the characterization of the complexes by the DFT calculations.

Table 3. Characteristics of the calculated complexes.

R-Br	$d_{Br\cdots N}$,[a] Å	$d_{X\cdots Br}^{com}/d_{X\cdots Br}^{sep}$ [b]	$-\Delta E$,[c] kJ mol^{-1}	Δq,[d] mē	λ_{max},[e] nm
$CH_2Br(NH_2)$	3.154	0.99	6.3	8.7	227
CH_3Br	3.004	1.00	10.9	15	224
CH_2BrF	2.949	1.00	13.7	20	223
CH_2Br_2	2.891	1.00	16.6	26	238
BrCCH	2.823	1.01	23.4	28	218
$C_6Br_2F_4$[f]	2.794	0.99	23.8	37	249
$C_2Br_2F_4$	2.785	1.00	24.5	41	249
$CHBr_3$	2.778	1.00	22.3	42	273
CBr_3CONH_2	2.727	1.01	24.0	54	269
CBr_3F	2.717	1.00	26.5	54	290
CBr_3COCBr_3	2.692	1.01	30.4	58	305
$CBrCl_3$	2.677	1.01	27.9	62	266
CBr_4	2.662	1.01	28.2	68	313
CBr_3CN	2.617	1.01	32.5	83	269
CBr_3NO_2	2.609	1.02	33.1	84	288
$CBr(NO_2)_3$	2.511	1.03	43.7	108	335
NBrSIM	2.439	1.04	43.5	129	235
NBrPIM	2.436	1.04	43.8	129	252
Br_2	2.350	1.05	53.3	213	303
NBrSAC	2.320	1.06	55.3	190	244
BrCl	2.309	1.06	61.9	221	281
BrF	2.213	1.06	94.9	228	232
DABCO-Br^{+g}	2.138	1.11	139.3	375	257
pyrazine-Br^{+g}	2.046	1.19	185.4	457	252
F_5Pyr-Br^{+g}	1.946	1.39	265.2	580	275

a) Distance between Br atom of R-Br and N atom of DABCO. b) Ratio of the covalent X-Br bond length in the halogen bonded R-Br electrophile to that in the individual one (see Table S3 in the ESI for details). c) $\Delta E = E_c - [E_{R\text{-}Br} + E_D]$ + BSSE, where E_C, $E_{R\text{-}Br}$ and E_D are the sum of the electronic and zero-point energies of the optimized adduct, R-Br and DABCO. d) Charge transfer from DABCO to R-Br (from NBO analysis). e) Absorption bands maxima (log ε ~ 3, see the ESI) from TD DFT calculations in acetonitrile. f) 1,4-dibromotetrafluorobenzene. g) Fragment of a cationic complex analogues to R-Br in the neutral complexes.

Similar to the experimental values in Table 2, the interatomic $d_{Br\cdots N}$ separations in the calculated R-Br·DABCO complexes in Table 3 cover the whole range from that of typical intermolecular associates to the traditional covalent bond length. The decrease of $d_{Br\cdots N}$ was accompanied by a progressive increase of the interaction strength, a gradual increase of charge transfer from DABCO to the R-Br electrophile (Fig. 4) and, in the stronger complexes, by an elongation of the covalent X-Br bond length (see the $d_{X\cdots Br}^{com}/d_{X\cdots Br}^{sep}$ ratios in Table 3). The close correlation between the $d_{Br\cdots N}$ and log ($-\Delta E$) values indicates an essentially exponential dependence of the interaction energies on the interatomic Br···N distances.

The TD DFT computations indicated that the nature of the electronic transitions observed in the UV-Vis spectra of the complexes is changing gradually along with the variation of the Br···N distances and charge delocalization. For the weaker complexes, e.g. [CBr_3F·DABCO], the major component of the intense optical transition involves electron transfer between the orbitals localized on the DABCO and $CFBr_3$ moieties (Fig. 5). In contrast, the intense optical transition in strong adducts, e.g. [Br_2·DABCO], involves electron movement between the orbitals delocalized over the whole complex.

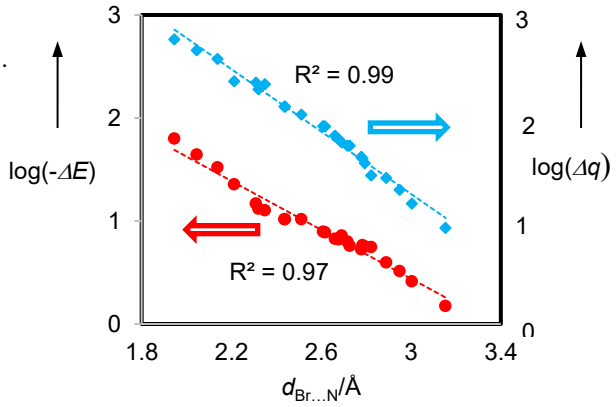

Figure 4. The dependencies of interaction energies (●) and charge transfer (♦) on interatomic Br···N distances.

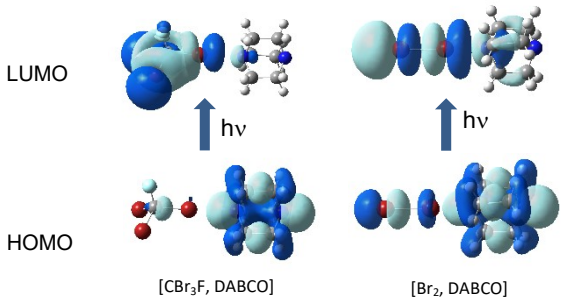

Figure 5. Electronic transitions responsible for the intense absorption bands in the UV-vis spectra of the [R-Br·DABCO] complexes.

In summary, experimental and computational studies on a series of R-Br·DABCO complexes revealed that at one extreme, Br···N distances (which were just ~10 % less than the van der Waals separations), interaction energies and charge transfer were similar to that typical of intermolecular associates. At the other endpoint, the series comprised very strong complexes in which Br···N distances were within 10% of a traditional covalent N–Br bond and charges were delocalized between R-Br and DABCO. The series also contains complexes with characteristics covering the whole range of values, eliminating any large changes and leaving no substantial gaps between successive entries. Thus, it demonstrates that the Br···N bond length and strength can change gradually from the values characteristic for intermolecular associates to that typical of a fully developed covalent bond. This continuum implies an intrinsic link between the limiting types of bonding and, therefore, the onset of covalency in intermolecular interactions. The gradual increase of its contribution results in the transformation of a (relatively weak) intermolecular interaction into a covalent bond. Finally, while this study was focused on Br···N bonding, preliminary data suggest that analogous continuums also exist for other series of halogen-bonded complexes (e.g. Br···Br or I···O). Ultimately, a gradual transition between intermolecular and covalent C–C bonds can be imagined based in a series of π-bonded and σ-bonded (ion-)radical dimers.

Acknowledgements We thank the National Science Foundation (grant CHE-1607746) for financial support of this work. We also thank Eric Loboda and Urszula Juszkiewicz for the initial UV-Vis study of the [R-Br·DABCO] complexes and Charlotte Stern for the X-ray analysis of CBr_3NO_2·DABCO crystals. X-ray measurements were supported by the NSF through the MRI Program (grant CHE 1625543, funding for the X-ray diffractometer).

Conflicts of interest

There are no conflicts to declare.

Notes and references

§ The predominance of 1:1 complexes was probably related to the fact that UV titrations were performed with excess of DABCO, while polarization of R-Br hindered bonding of the 2nd halogen-bond acceptor.[14]

‡ Crystallographic, data collection and structure refinement details are presented in the ESI. CCDC 1843782 (CBr_3CONH_2·DABCO), 1843783 ($CHBr_3$·DABCO), 1843784 (CBr_3F·DABCO), 1843785 ($(Br_2)_2$·DABCO) 1843786 ($CBrCl_3$·DABCO), 1843787 (DABCO-Br-DABCO), 1843788 (CBr_3NO_2·DABCO) contain the supplementary crystallographic data for this paper. These data can be obtained free of charge via www.ccdc.cam.ac.uk/data_request/cif.

1. a) L. C. Pauling, The Nature of the Chemical Bond and the Structure of Molecules and Crystals, 3rd ed.; Cornell University Press: Ithaca, NY, 1960. b) P. Gale and J. Steed, *Supramolecular Chemistry: From Molecules to Nanomaterials,* Ed. Wiley, Chichester, UK, 2012.
2. a) S. J. Grabowski, *Chem. Rev.*, 2011, ***111***, 2597–2625. b) H. Elgabarty, R. Z. Khaliullin, T. D. Kühne, *Nat. Commun.* 2015, ***6***, 8318. c) A. A. Grosch, S. C. C. van der Lubbe, C. Fonseca Guerra, *J. Phys. Chem. A* 2018, ***122***, 1813–1820. d) F. Weinhold, E. D. Glendening, *J. Phys. Chem. A* 2018, ***122***, 724–732.
3. a) Y. P. Yurenko, S. Bazzi, R. Marek, J. Kozelka, *Chem.-Eur. J.* 2017, ***23***, 3246–3250. b) C. Foroutan-Nejad, Z. Badri and R. Marek *Phys.Chem. Chem. Phys.* 2015, ***17***, 30670. c) R. Zhao, R.-Q. Zhang, *Phys. Chem. Chem. Phys.* 2017, ***19***, 1298–1302. d) Z. Mou, Y.-H. Tian, M. Kertesz, *Phys. Chem. Chem. Phys.* 2017, ***19***, 24761–24768.
4. a) V. Oliveira, D. Cremer, *Chem. Phys. Lett.* 2017, ***681***, 56–63. b) L. P. Wolters, F. M. Bickelhaupt, *ChemistryOpen* 2012, ***1***, 96–105. c) Wang, D. Danovich, Y. Mo, S. Shaik, *J. Chem. Theory Comput.* 2014, ***10***, 3726–3737. d) S. V. Rosokha, C. L. Stern, J. T. Ritzert, *Chem. Eur. J.* 2013, ***19***, 8774–8788. e) J. Thirman, E. Engelage, S. M. Huber, M. Head-Gordon, *Phys. Chem. Chem. Phys.* 2018, ***20***, 905–915. f) C. C. Robertson, R. N. Perutz, L. Brammer, C. A. Hunter, *Chem. Sci.* 2014, ***5***, 4179–4183.g) S. W. Robinson, C. L. Mustoe, N. G. White, A. Brown, A. L. Thompson, P. Kennepohl, P.D. Beer, *J. Am. Chem. Soc.,* 2015, ***137,*** 499-507. h) S. V. Rosokha, *Faraday Discuss.* 2017, ***203***, 315–332.
5. a) J. J. Novoa, P. Lafuente, R. E. D. Sesto, J. S. Miller, *Angew. Chem. Int. Ed.*, 2001, ***40***, 2540–2545. b) K. E. Preuss, *Polyhedron* 2014, ***79***, 1–15. c) Z. Cui, H. Lischka, H. Z. Beneberu, M. Kertesz, *J. Am. Chem. Soc.* 2014, ***136***, 12958–12965.
6. a) Y. Ishigaki, T. Shimajiri, T. Takeda, R. Katoono, T. Suzuki, *Chem* 2018, ***4***, 795–806. Schreiner, P. R.; Chernish, L. V.; Gunchenko, P. A.; Tikhonchuk, E. Y.; Hausmann, H.; Serafin, M.; Schlecht, S.; Dahl, J. E. P.; Carlson,R. M. K.; Fokin, A. A. *Nature* 2011, **477**, 308 − 311. b) A. Humason, W. Zou, D. Cremer, *J. Phys. Chem. A* 2015, ***119***, 1666–1682.
7. a) P. Metrangolo, P. Meyer, T. Pilati, G. Resnati, G. Terraneo, *Angew. Chem. Int. Ed.* 2008, ***47***, 6114–6127. b) G. Cavallo, P. Metrangolo, R. Milani, T. Pilati, A. Priimagi, G. Resnati, G. Terraneo, *Chem. Rev.* 2016, ***116***, 2478–2601. c) L. C. Gilday, S. W. Robinson, T. A. Barendt, M. J. Langton, B. R. Mullaney, P. D. Beer, *Chem. Rev.* 2015, ***115***, 7118–7195.
8. a) C.Prasang, A.C.Whitwood, D.W.Bruce Cryst.Growth Des. 2009, 9, 5319-5326 b) I.Nicolas, O.Jeannin, D.Pichon, M. Fourmigue *CrystEngComm, 2016, **18**, 9325-9333.* c) J.Mavracic, D.Cincic, B.Kaitner *CrystEngComm* 2016, **18** 3343-3346. d) R.Puttreddy, O.Jurcek, S.Bhowmik, T.Makela, K.Rissanen *Chem. Commun*. 2016 2338-2341. e) V. Stilinovic, G. Horvat, T. Hrenar, V. Nemec, D. Cincic, *Chem. Eur. J.* 2017, ***23***, 5244-5257.
9. S.C. Blackstock, J. P. Lorand, J. K. Kochi, *J. Org. Chem.* 1987, ***52***, 1451–1460.
10. a) E. H. Crowston, A. M. Lobo, S. Parbhakar, H. S. Rzepa, D. J. Williams, *J. Chem. Soc., Chem. Commun.* 1984, 276–278. b) K. Raatikainen, K. Rissanen, *CrystEngComm* 2011, ***13***, 6972–6977. c) M. Eraković, V. Nemec, T. Lež, I. Porupski, V. Stilinović, D. Cinčić, *Cryst. Growth Des.* 2018, ***18***, 1182–1190.
11. a) D. Cinčić, T. Friščić, W. Jones, *Chem. Eur. J.* 2007, ***14***, 747–753. b) A. K. Brisdon, A. M. T. Muneer, R. G. Pritchard, *Acta Cryst C,* 2015, ***71***, 900–902. c) L. Catalano, S. Perez-Estrada, H.-H. Wang, A. J.-L. Ayitou, S. I. Khan, G. Terraneo, P. Metrangolo, S. Brown, M. A. Garcia-Garibay, *J. Am. Chem. Soc.* 2017, ***139***, 843–848.
12. a) A. S. Micallef, R. C. Bott, S. E. Bottle, G. Smith, J. M. White, K. Matsuda, H. Iwamura *J. Chem. Soc., Perkin Trans.2* 1999**,** 65 -72. b) G. T. McCandless, D. Pangeni, F. R. Fronczek 2015 CCDC 1406559 (NBSUCA02) Private communication.
13. A. Bondi, *J. Phys. Chem.* 1964, ***68,*** 441-451.
14. Y. P. Nizhnik, A. Sons, M. Zeller, S.V. Rosokha *Cryst. Growth Des.* 2018, ***18***, 1198–11207.

